MODELING OF DROPLET MOVEMENT OVER SUPERHYDROPHOBIC SURFACE

نمذجة حركة قطرة على سطح سوبر هيدروفوبي

Mohamed-Nabil Sabry*, Mohamed ElNaggar*, and ElSayed ElGharieb**

* Mechanical Power Engineering Department, Faculty of Engineering, Mansoura University, Egypt
* E-mails: mnabil.sabry@gmail.com, naggarm@mans.edu.eg
** E-mail: el_gharib7@yahoo.com

ملخص

هذه الدراسة محاولة لعمل نموذج نظري لحركة قطرات السوائل على ما يسمى بالسطح السوبر هيدروفوبيك وهو السطح الذي تكون فيه الزاوية بين السطح والسائل عند نقطة التماس بينهما *180* درجة تقريباً. وهذا السطح يحتوي على عدد هائل من الخشونات الصغيرة جداً التي تقاس بوحدات الميكرون (جزء من الألف من المليمتر) أو النانو (جزء من المليون من المليمتر). هذه الخشونات والتي يوجد بها هواء تجعل من الصعب على السائل اختراق المسافات البينية الموجودة بين كل منها نظراً لأن قوة الشد السطحي سيكون لها التأثير الأكبر في هذه الأبعاد الصغيرة جداً، فيؤدي ذلك إلى تقليل مساحة تلامس السائل مع السطح الصلب كما يؤدي إلى وجود مساحة كبيرة في قاعدة القطرة يتلامس فيها السائل مع الهواء، مما يؤدي إلى تقليل قوة احتكاك السائل مع السطح وبالتالي تنزلق القطرة بسرعة كبيرة. وهذه النمذجة تتمثل في إيجاد معادلات تقريبية يمكن بها حساب القوى المختلفة المؤثرة علي القطرة في كل من حالتي السكون والحركة. هناك مجموعتان من القوى المؤثرة على القطرة سيتم إيجاد معادلات تقريبية لحسابهما أحدهما في الإتجاه العمودي علي السطح والأخرى في الإتجاه الموازي له. فالقوى العمودية على السطح تتمثل في قوة الشد السطحي وقوة الطفو الناتجة عن وجود أجزاء من الخشونات مغمورة في السائل. والقوى الموازية للسطح تتمثل في قوة الاحتكاك بين السائل والسطح وقوة إعاقة الهواء لحركة القطرة. إضافة لما سبق، هناك قوة أخرى ثابتة تؤثر على القطرة في كل من حالتي السكون والحركة وهي القوة اللازمة لدحرجة القطرة على هذه الأسطح وهي نوع من أنواع قوى الشد السطحي.

Abstract

Superhydrophobic surfaces are surfaces having a set of tiny protrusions (from micro to nano scale) capable of producing large "apparent" contact angles approaching 180°. Liquid droplet cannot wet these surfaces. Droplets will glide on the surface with a negligible friction. Some phenomenological models were proposed earlier to predict conditions for a droplet to be maintained at such a state without success. In this study, all interaction forces between droplet and wall are revisited. This includes forces exerted by the wall, either in the normal direction (surface tension and hydrostatic) or the tangential direction (frictional shear). This also includes drag force of surrounding air as the droplet moves. For all these forces, simplified phenomenological models are proposed here, based on either order of magnitude analysis or detailed 3D simulation to investigate fluid behavior in such complicated flow fields. Obtained simple forms were successful in reproducing, at least qualitatively, observed behavior.

Accepted March 31, 2012

NOMENCLATURE

A_{proj}	Projected area facing fluid flow
C_D	Drag coefficient
E_b	Energy required to create free surface
F_A	Overall air drag force
F_b	Force required to create free surface
F_D	Drag force over one protrusion
F_h	Hydrostatic force
F_s	Surface tension force in the normal direction to the tilted plane
g	Gravitational acceleration
N_p	Number of protrusions lifting the droplet
p	Distance between any two successive protrusions
P_{amb}	Ambient pressure
P_{drop}	Pressure inside the droplet
r, z	Cartesian coordinates
R	Local radius of curvature
R_0	Radius of curvature at the symmetric line
R_b	Radius of droplet base
Re	Reynolds number
R_s	Radius of the perfect spherical droplet
R_w	Radius of the wet area of one protrusion
s, ϕ	Intrinsic coordinates
S_D	Average shear stress under droplet bottom
t	Time
u	Droplet velocity at the wall due to partial slip condition
u_∞	Droplet velocity
v	Air velocity
α	Angle between the liquid and the horizontal at the contact point for the protrusion
β	Contact angle for liquid droplet on a perfect flat surface
δ	Slip length for the superhydrophobic surface
$\Delta\rho$	Droplet density minus ambient fluid density
θ_o	Maximum angle of static equilibrium
μ	Droplet liquid viscosity
ρ	Air density
ρ_d	Density of the droplet liquid
σ	Surface tension coefficient

1. INTRODUCTION

Liquid droplets when deposited on a surface can either wet it (i.e. spread on it) if the contact angle $\beta < 90°$ or remain grouped with a minimum wetting area if $\beta > 90°$. The former case is called hydrophilic, the latter hydrophobic (Fig. 1). Contact angle depends on the combination of the three materials composing the solid surface, the droplet liquid and surrounding fluid. The greater the contact angle, the less real contact area will be observed between droplet and solid surface. Recently, a large number of publications were devoted to the so-called superhydrophobic surfaces [1], for which the "apparent" contact angle is much greater than 90° approaching 180°. Although contact angle is a property of the combination of three materials, attaining superhydrophobic state was mainly due to a modification of surface quality, almost regardless of the nature of materials involved [2].

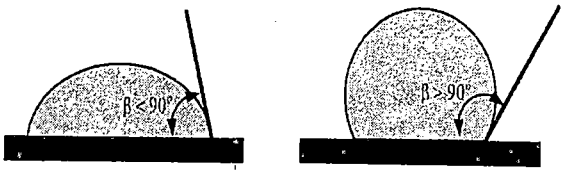

(a) Hydrophilic (b) Hydrophobic

Figure 1. Contact angle cases

Interest in superhydrophobic surfaces is due to the numerous applications they may have. When the actual contact area between solid and liquid becomes so negligible, the droplet will glide over the surface with almost zero frictional resistance. Self-cleaning surface is one of the very interesting applications. For example, it can be used to maintain wind turbine efficiency by preventing dirt accumulation [3]. Tiny droplets that may be present naturally (due to dew for instance) or artificially (a very small amount of

droplets from an atomizer) will easily glide over the surface scanning it and collecting dirt in the same time. This is the principle behind the self-cleaning of lotus leaves. Superhydrophobic phenomenon is sometimes referred to as the lotus effect [4].

Another important potential application is the drag reduction for liquid transportation over long distances, which may result in large energy savings [5].

Lab-on-a-chip is another promising application in which tiny droplets are manipulated over an electronic chip surface [6]. Droplet moves under the action of an electric field created by the chip. Droplets can be mixed with other fluids, heated and cooled to perform different biological tests. Evidently, drops should be non-wetting to prevent liquid loss as well as to reduce electric field intensity needed to move it.

The aim of the present paper is to propose a simplified phenomenological model of droplet dynamics over a superhydrophobic surface. Conditions for this phenomenon to take place, i.e. for the droplet to be "lifted" over the surface, as well as related frictional and drag forces for a moving droplet are studied. The phenomenological model is based on order of magnitude analysis as well as detailed simulation of relevant test cases. The outcome of the present study is to get a model "structure" that mimics, at least qualitatively, actual droplet behavior. Few adjusting parameters can be easily included to fit experimental data, provided a sufficient number of validated test experiments were obtained. Model structure has already shown good qualitative behavior, as compared to published observations, unlike other phenomenological models suggested in literature. This validates the proposed model structure. Adjusting parameters to quantitatively fit test results would require a systematic test campaign, which may be the object of a future work. In the present study, a certain number of experiments were conducted for the sake of proof of concept.

In the sequel, a static droplet is first studied to establish conditions of equilibrium. A sessile droplet is considered over a superhydrophobic surface composed of tiny surface irregularities at the micro or nano scales. This is followed by the study of moving droplets. An estimate of wall frictional resistance opposing droplet movement is made. It is based on a fine analysis of the movement of droplet bottom layer, just around surface irregularities. A model for drag forces exerted by surrounding air is also proposed, based on detailed analysis of coupled flow fields inside and outside the droplet. Lastly, an experimental setup to validate the concept is described.

2. SESSILE DROPLET

2.1 Sessile Droplet Shape

For a surface to be superhydrophobic, it has to have a multitude of tiny surface roughness elements, which would be able to keep the droplet in a Cassie-Baxter state (Fig. 2.a) above protrusions, much as a "fakir" can sleep on a bed of nails, instead of the Wenzel state, (Fig. 2.b) where droplet base penetrates inside craters. Superhydrophobic property is obtained by creating miniature roughness at nano to micro scales.

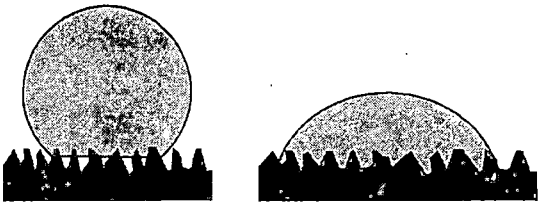

(a) Cassie-Baxter state (b) Wenzel state

Figure 2. Droplet states over a rough surface

A sessile droplet is a droplet that is at rest under the action of gravity and surface tension forces only, in addition to the reaction of a wall supporting the droplet.

The sessile droplet is no longer being spherical, but the height is a bit less than its width at a ratio that depends on the Bond number. The droplet is considered as axisymmetric, because all acting forces are so. Figure 3 sketches the shape of a sessile droplet. Cylindrical coordinates r, z are used (z-axis points vertically downwards) with an origin at droplet top. It is also useful to define intrinsic coordinates s and ϕ (arc length and tangent angle with r axis, respectively) as shown in the figure. Intrinsic coordinates s and ϕ can be expressed in terms of polar coordinates r, z by the well-known relations:

$$ds=\sqrt{(dr)^2+(dz)^2}\ ;\ \tan\varphi=dz/dr \quad (2.1)$$

Obviously, the local radius of curvature R at any point on the surface is given by: $R = ds/d\phi$.

The pressure difference at any surface point between inside and outside fluids is governed by the static force balance across the interface:

$$P_{drop} - P_{amb} = \sigma[1/R + sin(\phi)/r] \quad (2.2)$$

where P_{drop} and P_{amb} are the droplet and ambient pressures, and σ is the surface tension coefficient.

The pressure in both fluids increases as we go from the top of the droplet (at which $R = R_0$) downwards because of gravity. Droplet density is higher (otherwise, it would have floated up). Droplet density minus ambient fluid density is denoted as $\Delta\rho$. The pressure difference increases by moving downwards due to density difference, i.e. the radius of curvature decreases going downwards. This shape is governed by the differential equation:

$$2\sigma/R_0 + \Delta\rho\, g\, z = \sigma[d\phi/ds + sin(\phi)/r] \quad (2.3)$$

where $2\sigma/R_0 = (P_{drop} - P_{amb})|_{z=0}$ and g is the gravitational acceleration. The droplet shape has the initial condition:

$$\text{At } r = 0;\ z = 0 \quad (2.4)$$

The differential equation (2.3) can be easily integrated to get the sessile droplet shape. Integration continues until the interface tangent becomes horizontal again. At that point, the surface lies on the wall, where the inside pressure is counterbalanced by reaction. Hence, the interface is flat (or at least flat "on the average" due to surface irregularities). Thus, the integration of the differential equation gives the droplet base area that lies on the wall. A typical sessile droplet profile is given in Fig. 4. The pressure exerted on (or by) the wall is calculated by dividing the droplet weight by the base area of droplet profile.

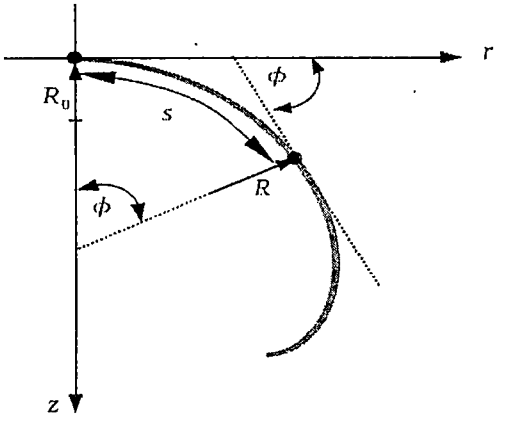

Figure 3. Sessile droplet modeling

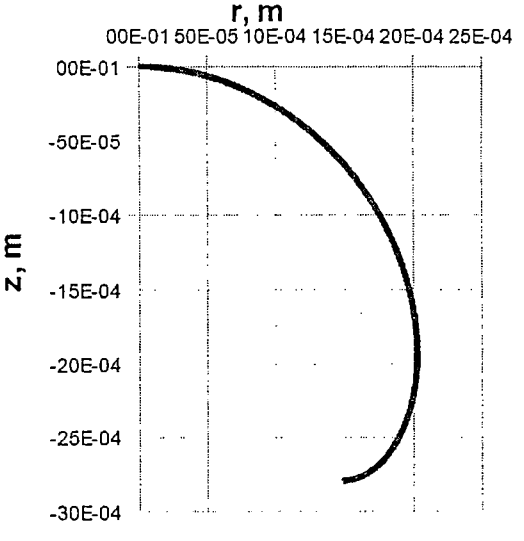

Figure 4. A typical sessile droplet shape

The water solutions at different volumes shows that the base radius is

always around 70% of the original perfectly spherical droplet radius before being deposited on the wall. This ratio is taken as an order of magnitude to proceed further in this study.

2.2 Forces Exerted by the Wall on a Sessile Droplet

The details of interactions between droplet base and one small scale protrusion are examined by changing the length scale. When a droplet is first deposed on a wall, it starts touching the upper points of surface protrusions. These points have zero area and cannot therefore exert any force on the droplet. Hence, the droplet will fall for a certain distance. As the droplet falls, protrusions will penetrate into the droplet causing two kinds of forces: (a) Surface tension force, and (b) Hydrostatic force.

The surface tension force exerts at the triple interface line where solid wall, droplet liquid and outside fluid meet.

The hydrostatic force is due to protrusions penetration into a zone of fluid pressure gradient. In fact, this hydrostatic force is simply the weight of droplet fluid having the same volume as that displaced by the protrusion. The total force can be easily estimated using Archimedes Principle.

Both forces increase as the protrusions penetrate inside the droplet. They will continue increasing until either they are able to counterbalance droplet weight, giving the Cassie-Baxter state, or the droplet reaches the bottom without being counterbalanced, which corresponds to the Wenzel state.

The conditions for a Cassie-Baxter (Fig. 2.a) state are obtained by the estimation of surface tension and hydrostatic forces. First, for simplicity, assume that the superhydrophobic surface contains disconnected regularly distributed micro rough elements (protrusions); the distance between any two protrusions is p, Fig. 5. Second, suppose that the droplet disposed on a tilted superhydrophobic surface and it rests on the surface with a base area of radius R_b, Fig. 6. Third, knowing that the droplets tend to roll on the superhydrophobic surface rather than slide, [7], the energy required to roll the droplet on the superhydrophobic surface can be approximately calculated by imagining finite distance movement of the droplet. This movement creates a new water-air interface on the trilling edge. The finite distance can be supposed for simplicity the virtual distance $2R_b$.

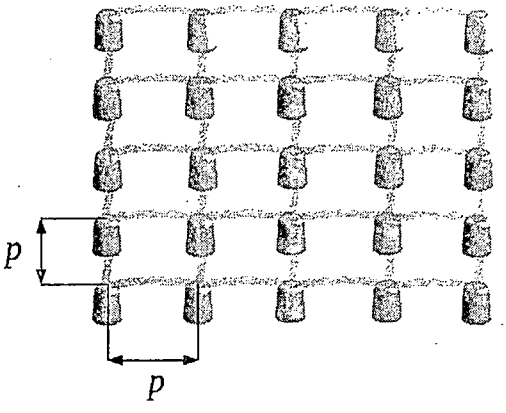

Figure 5. Regularly distributed micro rough elements

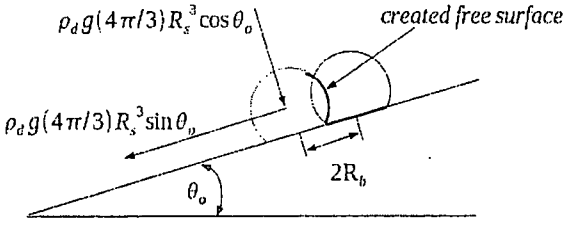

Figure 6. Surface created after rolling virtual distance equals $2R_b$

The energy required to create the new surface, E_b, is given by:

$$E_b = \pi R_w^2 \, \sigma \, N_p \qquad (2.5)$$

where R_w is the radius of the wet area of protrusion, Fig. 7, and N_p is the number of protrusions lifting the droplet defined as the base area divided by the pitch area surrounding one protrusion:

$$N_p = \pi R_b^2 / p^2 \qquad (2.6)$$

The force F_b is calculated by dividing the energy by the virtual distance:

$$F_b = \pi R_w^2 \sigma N_p / (2R_b) \quad (2.7)$$

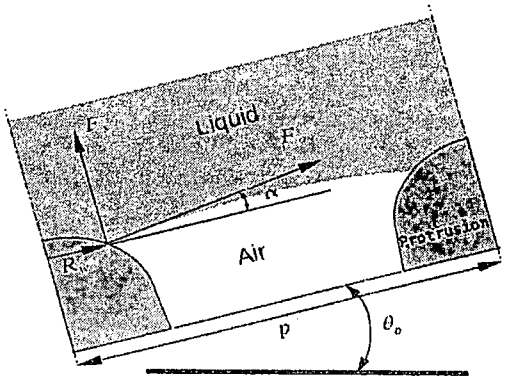

Figure 7. Droplet bottom over a protrusion

Substituting from Eq. (2.6) into Eq. (2.7) and using the approximation $R_b \cong 0.7\ R_s$, one get:

$$F_b = 0.35\pi^2 R_w^2 \sigma R_s / p^2 \quad (2.8)$$

The static balance for the droplet in the direction of the tilted plane gives:

$$F_b = \rho_d g (4\pi/3) R_s^3 \sin \theta_o$$
$$= 0.35\pi^2 R_w^2 \sigma R_s / p^2 \quad (2.9)$$

where θ_o is the maximum angle of static equilibrium and it is measured experimentally, and ρ_d is the droplet density.

Simplifying Eq. (2.9), the value of R_w is obtained as:

$$R_w^2 = 1.2 \rho_d g R_s^2 p^2 \sin \theta_o / \sigma \quad (2.10)$$

The surface tension force in the normal direction to the tilted plane F_s:

$$F_s = 2\pi R_w \sigma N_p \sin \alpha \quad (2.11)$$

The angle α can be calculated by making a static balance for the droplet in the direction of the normal to the tilted plane:

$$\rho_d g (4\pi/3) R_s^3 \cos \theta_o = 2\pi R_w \sigma N_p \sin \alpha \quad (2.12)$$

Thus,

$$\sin \alpha = 0.433 \rho_d g R_s \cos \theta_o p^2 / (R_w \sigma) \quad (2.13)$$

The hydrostatic force, F_h, is the weight of droplet liquid that would have filled the displaced volume, i.e. the shaded spherical cap, Fig. 8. It is exactly similar to the force required to lift a floating body on water, Fig. 8. For simplicity, the assumption that the volume of the cap is far smaller than the half of the volume of the sphere of radius R_w, Fig. 8, yields:

$$F_h < \rho_d g (2\pi/3) R_w^3 N_p \quad (2.13)$$

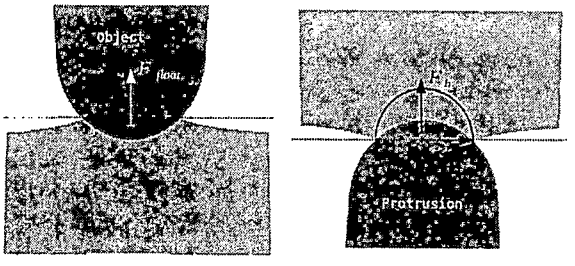

Figure 8. Calculation of the magnitude of hydrostatic forces

The ratio of hydrostatic force to surface tension force can be estimated as:

$$F_h / F_s < R_w^2 \rho_d g / (3 \sigma \sin \alpha) \quad (2.14)$$

Taking some realistic values as ρ_d = 1000 kg/m^3, $R_s = 1.7 \times 10^{-3}$ m, $\sigma = 0.075$ N/m, $p = 10^{-5}$ N/m^2, it appears that this ratio is of the order of $< 4.15 \times 10^{-5}$. Hence, the hydrostatic forces can be safely neglected.

3. WALL SHEAR AND SLIP CONDITION

Experimental observations indicate an extremely low resistance to droplet movement and that droplets retain their integrity for a long time, Fig. 9, suggesting that the no slip condition; usually applied on wall boundaries; is rather not plausible. For modeling the slip phenomenon, the ultra small analysis scale of droplet base reacting with a wall protrusion is used and the protrusions with a flat circular cap of radius R_w is assumed. Any other cap shape

would behave in a similar way to results of this section. In fact, since the contact area is so small, with a very small subtended angle, cap precise shape should be rather irrelevant.

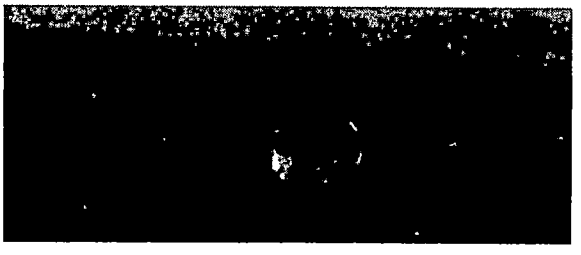

Figure 9. A typical large droplet (5 mm diameter) over a superhydrophobic surface (obtained by covering a flat metallic surface with soot)

Liquid base has a very small contact area with solid walls. While conditions above the wet area can be assumed to be of no-slip type, this cannot be assumed for the other portion of droplet base area. Liquid faces there an air layer of very small viscosity working as a cushion reducing wall friction. Therefore, it is reasonable to assume that a full slip condition, i.e. a zero wall shear, prevails over the air cushion. Figure 10 shows the flat cap problem geometry. The droplet base velocity parallel to walls is u, and at points sufficiently far from a protrusion, it is close to the average droplet advance velocity, u_∞.

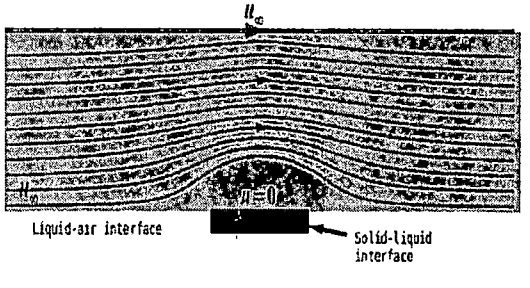

Figure 10. Flat cap problem geometry

As liquid approaches the protrusion, u gradually diminishes to reach zero at the upstream side of the protrusion, where a no-slip condition has been imposed. Liquid will thus acquire a vertical velocity component v normal to solid walls to satisfy continuity. The same will happen in a reverted way at the downstream side of the protrusion. A normal velocity component towards the wall will appear to satisfy continuity. Liquid wall tangential velocity u will increase gradually from zero at the last point over the protrusion to u_∞ as the liquid progress over the air cushion. Hence, the liquid streamlines are expected to behave as if they were avoiding an obstacle having a concave shape. This means that, at least qualitatively, the protrusion cap shape (flat or hemispherical) does not really matter. In fact, for the case of a flat cap, the liquid trapped between the free stream avoiding the discontinuity created by the protrusion and protrusion cap has a very small thickness. It will hence offer almost the same resistance to free stream as a solid hemispherical cap.

The numerical results of a detailed finite volume simulation of flow over a flat cap protrusion obtained using the open source Computational Fluid Dynamics software Open Foam [8], Fig. 11, confirm this argument.

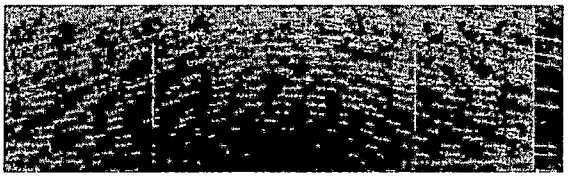

Figure 11. Simulation results for the flat cap problem obtained by Open Foam

Hence, the resistance is expected to be of the same order as drag force of a fluid going around a set of obstacles. Since the tangential velocity of liquid droplet bottom above air cushion is almost u_∞, and since protrusions are so wide apart as compared to the size of the wet area over the cap, the liquid streamlines can be approximated by those of the upper half of a free stream flowing over a perfect sphere with diameter $2\,R_w$. The small value of the diameter clearly indicates that the flow will be laminar with a very small Reynolds number

Re. The drag coefficient C_D for this type of flow is known to be:

$$C_D = 24 / Re \tag{3.1}$$

i.e., the drag force F_D over one protrusion is:

$$F_D = 3\,\pi\,\mu\,R_w\,u_\infty \tag{3.2}$$

Assuming that the streamlines over different protrusions do not interact and knowing that the area associated to one protrusion is p^2, then the average shear stress over droplet bottom is:

$$S_D = 3\,\pi\,\mu\,R_w\,u_\infty / p^2 \tag{3.3}$$

Now, zooming out to focus on a large base area of length scale much larger than p, and assuming that both droplet base and wall are perfectly flat because the surface geometrical irregularities cannot be noticed at that level, although their mechanical effect is still there. The effect is to have both a nonzero average droplet base velocity as well as a nonzero average shear stress over the same area. Evidently, they are proportional to each other. This is a classical partial slip case, Fig. 12, which is typically modeled by a boundary condition of the type:

$$u = \delta\,\partial u/\partial y \tag{3.4}$$

where δ is the so-called slip length.

Comparing Eqs. (3.3) and (3.4), the slip length is written as:

$$\delta = p^2 / (3\,\pi\,R_w) \tag{3.5}$$

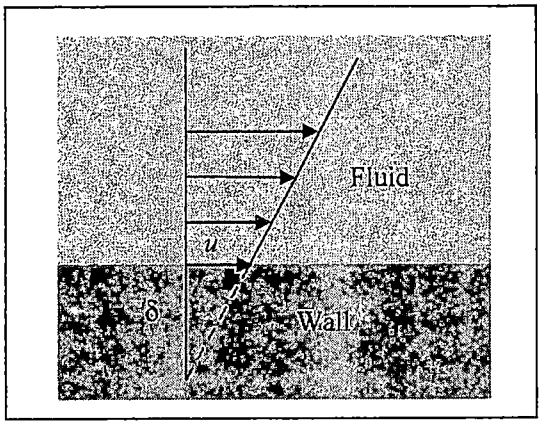

Figure 12. Partial slip model

4. AIR DRAG EXERTED ON A MOVING DROPLET

Droplet movement is not only opposed by wall shear stress, which proved to be rather negligible, but also opposed by air drag, like any moving object.

Drag models usually take the form:

$$F_A = C_D\,A_{proj}\,\rho\,v^2 / 2 \tag{4.1}$$

where F_A is the overall drag force, and A_{proj} is the projected area facing fluid flowing at a velocity v and fluid density ρ.

Drag coefficient depends on droplet shape, flow regime (laminar or turbulent), and boundary condition over droplet surface. Consider for simplicity that the droplet was replaced with a rigid body that is almost spherical. In this case, air drag would be given by Eq. (4.1) with a known value of C_D which would depend on the regime (laminar/turbulent). The real case, of a non-rigid droplet, would differ from the rigid one in two respects. First, boundary condition on droplet surface would allow a non-zero relative velocity between droplet surface and average droplet velocity. This tends to get a lower drag coefficient. Second, the droplet shape is continuously oscillating during its movement. This would tend to increase the drag coefficient. The actual value would be difficult to predict.

Drag force can be obtained either by experiments or by a detailed 3D simulation. The value of drag force given by Eq. (4.1), with the drag coefficient of a rigid sphere is expected though to give the correct order of magnitude.

For simulation to be realistic, it must allow droplet liquid to have an internal velocity field. It must also allow droplet shape to vary and to track droplet interface movement. These features are present in the open software package Open Foam, available in the public domain.

Droplet movement was simulated numerically according to the following scenario. First, a droplet is gently deposited from a small height above a horizontal superhydrophobic wall under the action of its weight. Simulation extends until the droplet is almost at rest. In a second phase, air is blown parallel to the wall, with a constant uniform shear profile. Air has a zero velocity at the wall (no-slip condition). The droplet will start moving with an increasing velocity, which was recorded at each time step.

Problem parameters are:

- Original spherical droplet diameter is 4 mm,
- Sessile droplet height is 2.8 mm,
- Apparent wall contact angle is 170°,
- Domain height is 6 mm,
- Air velocity at domain top is 1.7 m/s, decreasing linearly to reach zero at domain bottom,
- Domain length (along air flow direction) is 15 mm,
- Domain depth is 10 mm,
- Air and water densities are 1 and 1000 kg/m^3, respectively, air and water kinematic viscosities are 1.48×10^{-5} and 10^{-6} m^2/s, respectively, surface tension coefficient is 0.07 N/m.

It has been observed that the sessile droplet, when first deposited, can hardly remain stable in its place. It bounces easily from the surface and takes a long time before settling, which has been also observed in the literature as well as in the public videos. Droplet oscillations never completely die out. Simulation in the second phase has started with some residual oscillations.

When air velocity field is introduced, the droplet starts moving under the action of air drag. Time evolution of velocity, Fig. 13, allows getting acceleration by numerical differentiation and hence the inertia force (mass x acceleration). Shear stress beneath the droplet is directly proportional to droplet velocity, Eq. (3.3), and hence can be easily obtained. Shear force is equal to the shear stress multiplied by base area, Eq. (3.2), which changes with time due to droplet oscillations. Adding inertia to shear, the total driving drag force is obtained.

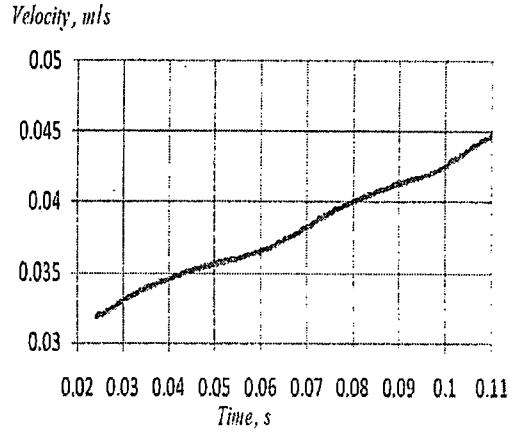

Figure 13. Instantaneous droplet velocity

This force is substituted in the classical drag model, Eq. (4.1). The velocity appearing in this expression is the average free stream air velocity across droplet height minus the average droplet velocity. The projected area A_{proj} stands for droplet cross-sectional area by a vertical plane passing by its center. Using droplet base and projected areas from simulation results, shear model developed above and classical drag model, the instantaneous drag coefficient, Fig. 14 (dotted line), is obtained.

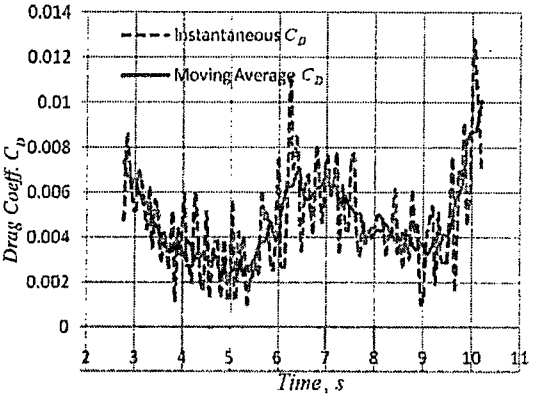

Figure 14. Instantaneous drag coefficient

Figure 14 shows three different time scales. The first corresponds to very fast oscillations of a period ~ 1 ms. These oscillations are mainly numerical. They are due to the volume of fluid (VOF) method which is characterized by a fixed mesh. Each cell contains either liquid, gas or a mixture, in case the liquid/gas interface crosses cell boundaries. Calculated cross-sectional or base droplet areas manifest some discontinuities when the interface leaves a cell and crosses a neighboring one. These oscillations can be easily filtered by applying a moving average drag coefficient, Fig. 14 (solid line).

The second time scale is related to droplet oscillations. These oscillations are physical and correspond to droplet natural frequency of oscillations. They may be of interest by their own to study droplet fragmentation after a violent shock. However, if our interest was in droplet movement as a whole, then their filtration may be needed.

Instantaneous C_D values were developed over Legendre polynomials to detect different components of this chaotic signal. It appears that the average value (order zero) plus only 1 component (order 4) carry most of the signal, Fig. 15. The first five terms are also plotted to show that signal energy in other terms is small. In fact, all other signal components appear as a white noise. The average value of C_D is 0.0047. Droplet oscillation causes fluctuations in C_D to reach at most 0.01. This is a very reasonable value, as it is lower than but comparable to C_D of air flowing around a solid sphere. The latter is equal to $24/Re$, Eq. (3.1), for laminar flow, i.e. ~ 0.015 in the studied case.

Figures 16 to 18 give the simulation results for the advancing droplet at sample times that show clear oscillations.

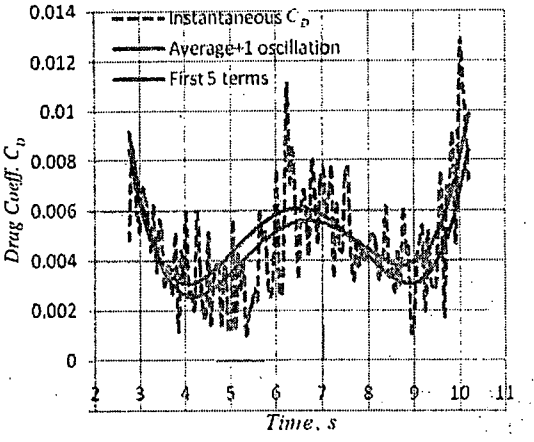

Figure 15. Filtered instantaneous droplet velocity

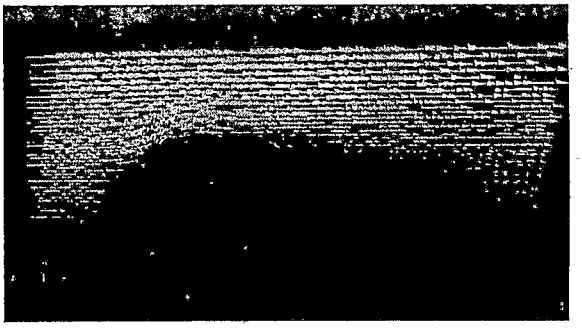

Figure 16. Droplet position and shape at t = 36 ms

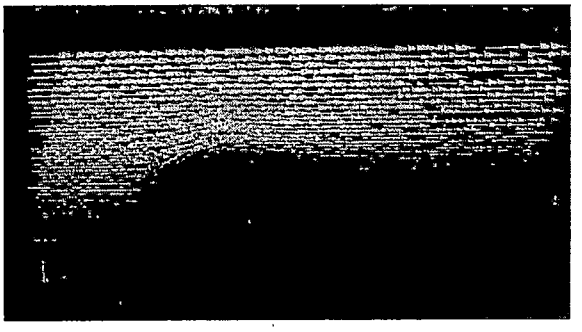

Figure 17. Droplet position and shape at t = 66 ms

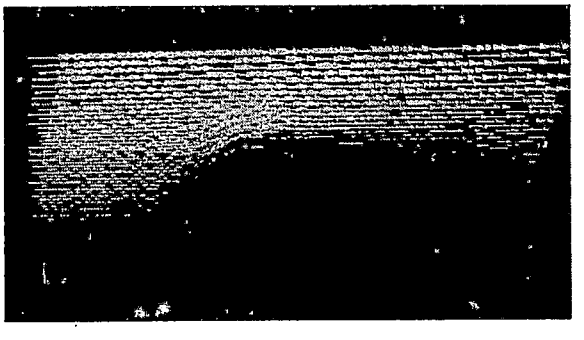

Figure 18. Droplet position and shape at t = 84 ms

Hence, a simplified model for drag coefficient of outside air opposing droplet movement can be obtained by modifying that of a spherical droplet in laminar flow, Eq. (3.1):

$$C_D = c_c \, 24 / Re \qquad (4.2)$$

where c_c is a correction coefficient and its value is less than one.

5. CONCLUSION

Droplet dynamics over a superhydrophobic surface was examined in all its aspects. A phenomenological model was derived for all relevant forces. The objectives of these models were multiple. First, they help understanding underlying physics. Second, they can provide correct order of magnitudes. Last, but not least, adjusting parameters can be easily inserted to fit experimental data, in order to get reliable results that are more accurate.

The forces acting on the sessile droplet include:

- Surface tension forces: Droplet/surface contact area is composed of a huge number of small areas, one on each protrusion. The periphery of these areas is large compared to its area due to its small size. A simple model was obtained to predict conditions under which droplet can be maintained by protrusions in a free gliding state.
- Hydrostatic forces: These forces are proportional to the volume that is displaced by protrusions which proved to be negligible.
- Shear resistance at droplet bottom: Since contact areas are small, with an air cushion under the droplet that occupies most of droplet base, a slip model was developed that accounts for this very small resistance. Arguments used to build the model verified by detailed simulation.
- Drag force exerted by surrounding air: Detailed 3D simulation were performed for a moving droplet showing that the drag coefficient is less than that of air flowing over a solid sphere but of the same order of magnitude.

References

[1] Maynes, D., Jeffs, K., Woolford, B., and Webb, B.W., "Laminar Flow in a Microchannel with Hydrophobic Surface Patterned Microribs Oriented Parallel to the Flow Direction", *Physics of Fluids*, Vol. 19, 2007, 093603.

[2] Rothstein, J.P., "Slip on Superhydrophobic Surfaces", *Annual Review of Fluid Mechanics*, Vol. 14, 2010, pp. 89-109.

[3] Khalafallah, M.G., and Koliub, A.M., "Effect of Dust on the Performance of Wind Turbines", *Desalination*, Vol. 209, 2007, pp. 209-220.

[4] Barthlott, W., and Neinhuis, C., "Purity of the Sacred Lotus, or Escape from Contamination in Biological Surfaces", *Planta*, Vol. 202, 1997, pp. 1-8.

[5] Davies, J., Maynes, D., Webb, B.W., and Woolford, B., "Laminar Flow in a Microchannel with Superhydrophobic Walls Exhibiting Transverse Ribs", *Physics of Fluids*, Vol. 18, 2006, 087110.

[6] Kumari, N., Bahadur, V., and Garimella, S.V., "Electrical Actuation of Dielectric Droplets", *Journal of Micromechanics and Microengineering*, Vol. 18, 2008, 085018.

[7] Mahadevan, L., and Pomeau, Y., "Rolling Droplets", *Physics of Fluids*, Vol. 11, No. 9, 1999, pp. 2449-2453.

[8] OpenCFD Limited, "OpenFOAM The Open Source CFD Toolbox User Guide", *Free Software Foundation*, Version 1.6, 2009.